



Laboratory tests of Hidrostal pump

UNIVERSITE DE LIEGE

MAY 2023



Table of contents

Table of contents.....	1
1 Introduction.....	2
2 Pump 4: Hidrostal F10K-HLT1 + FEVB4-GSEK1CC + ND1A8EA-20.....	2
3 Experimental observation	4
3.1 VFD provided by CRT.....	4
3.2 Soft starter	5
4 Computational results.....	6

This document is an add-on to the report “Assessment of the performance of large-capacity pumps used in waterways: experimental tests and computational modelling” which constitutes deliverable WP.11.2.1 of the Interreg NWE Green WIN project.

1 Introduction

A suitable tool to evaluate the actual on-site energy efficiency of pumping systems used in waterways is missing. Indeed, pump manufacturers generally provide detailed information on a curve of pump efficiency at nominal rotation speed only. In contrast, no or little information is available concerning off-design pump operation for varying speed, while variable speed drives are known to enable increasing the overall efficiency of the pumping system, which is precisely what matters for the end-users. A hybrid modelling approach has been developed in the Interreg NEW Green Win project. It involves a large experimental test bench used for calibrating a computational model of the whole system, including the motor, the pump and the hydraulic setting.

In this report, we detail the experimental and computational results obtained for the pump Hidrostral F10K-HLT1 + FEVB4-GSEK1CC + ND1A8EA-20 provided by Canal River Trust (CRT).

2 Pump 4: Hidrostral F10K-HLT1 + FEVB4-GSEK1CC + ND1A8EA-20

The main operating characteristics of the pump, according to the manufacturer, are listed in Table 1. Technical drawings of the pump are displayed in Figure 2.1. Pump curves provided by the manufacturer datasheet are also shown in Figure 2.1. Figure 2.2 shows the pump installed in the tank. This pump was tested according to Testing procedure n°3.

Flow rate	200 l/s	Nominal voltage	400 V
Head	10 m	Nominal frequency	50 Hz
Operating speed	1480 RPM	Nominal electrical power	37 kW
Absorbed power	27 kW	Nominal current	68 A
Efficiency	81.3 %	Nominal efficiency	NC
Number of pair of poles	2	Nominal power factor	0.85

Table 1 : Operating characteristics of the Hidrostral pump.



Figure 2.2: (a) Hidrostal pump placed inside the tank and (b) associated VFD

3 Experimental observation

In this section, the results of the test bench are displayed for two different control types / strategies: a dedicated VFD provided by CRT and a soft starter.

Note that direct online (DOL) starting was not tested. Indeed, with DOL, the current can increase momentarily from 7 to 10 times the nominal current. Some electrical components may not accept that sudden increase such as fuse and lead to electric damages. From a mechanical perspective, it means that the pump pressure and flow rate start suddenly to increase with a large rate and this can lead to considerable vibrations and damages. Furthermore, no additional scientific information would be obtained on such experiments since all measurements are taken in steady operation. We just would retrieve the 50 Hz results displayed in Figure 3.1. For those reasons, the Direct On Line (DOL) starting was not performed on the Hidrostal pump.

3.1 VFD provided by CRT

A total of 152 operating points ($N_p = 152$) were measured during the tests of the Flygt pump with a dedicated VFD provided by CRT (Figure 3.1). The head-(flow rate) curve with a 50 Hz motor excitation deviates from the manufacturer datasheet (displayed in dashed line) by no more than 1 meter. This difference may originate from some variability in pump manufacturing.

The efficiency communicated by the manufacturer (Figure 3.1.b) represents solely the pump efficiency (separated from the effect of motor losses). By multiplying the maximum efficiency at 50 Hz according to the manufacturer (81%) by the nominal motor efficiency (assumed equal to 90%), the resulting combined efficiency of the motor-pump system may be estimated at 73%, which is 5% above the observed maximum efficiency 68% (grey values). This 5% difference may be explained by both some variability in the pump manufacturing process and, to a greater extent, by a slight off-design operation of the motor (being mostly operated at 30kW instead of 37kW, i.e. with a load of 81%). Assuming it may result in a pump efficiency of 79% and motor operating at a plausible value of

87% efficiency, the resulting combined efficiency would be 68.7%, which corresponds to the experimental observations. The efficiency of the variable frequency drive (VFD) increases as the frequency rises and is over 90% for the CRT Hidrostral drive when the frequency is greater than 25 Hz. In the sake of energy-efficiency, it is not advised to operate it at a frequency below 25Hz.

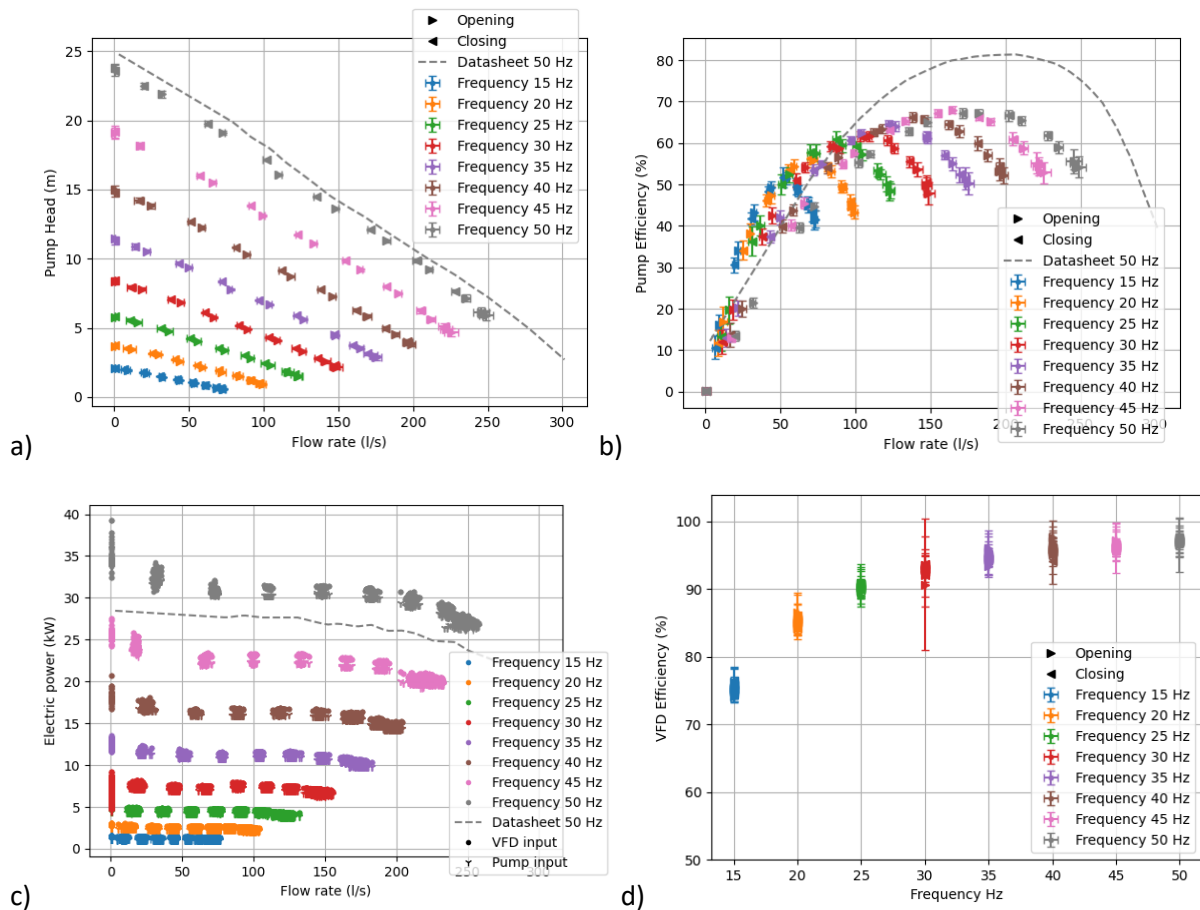


Figure 3.1: Experimental results of testing procedure n°3 compared to datasheet for the Hidrostral pump: (a) head-(flow rate) curve; (b) overall pump efficiency curve; (c) Electric input powers to the VFD and to the pump and (d) VFD efficiency

3.2 Soft starter

As shown in Figure 3.2, the results obtained using a soft starter instead of a VFD are very similar those obtained with a VFD set to 50 Hz. The efficiency of the VFD at 50 Hz and the efficiency of the soft starter appear equivalent. Indeed, the main purpose of a soft starter is to act on the dynamic behaviour of the pump which helps on both mechanical and electrical sides to avoid sudden and temporary increases in pressure, flow rate and current and thus prevent from potential damages.

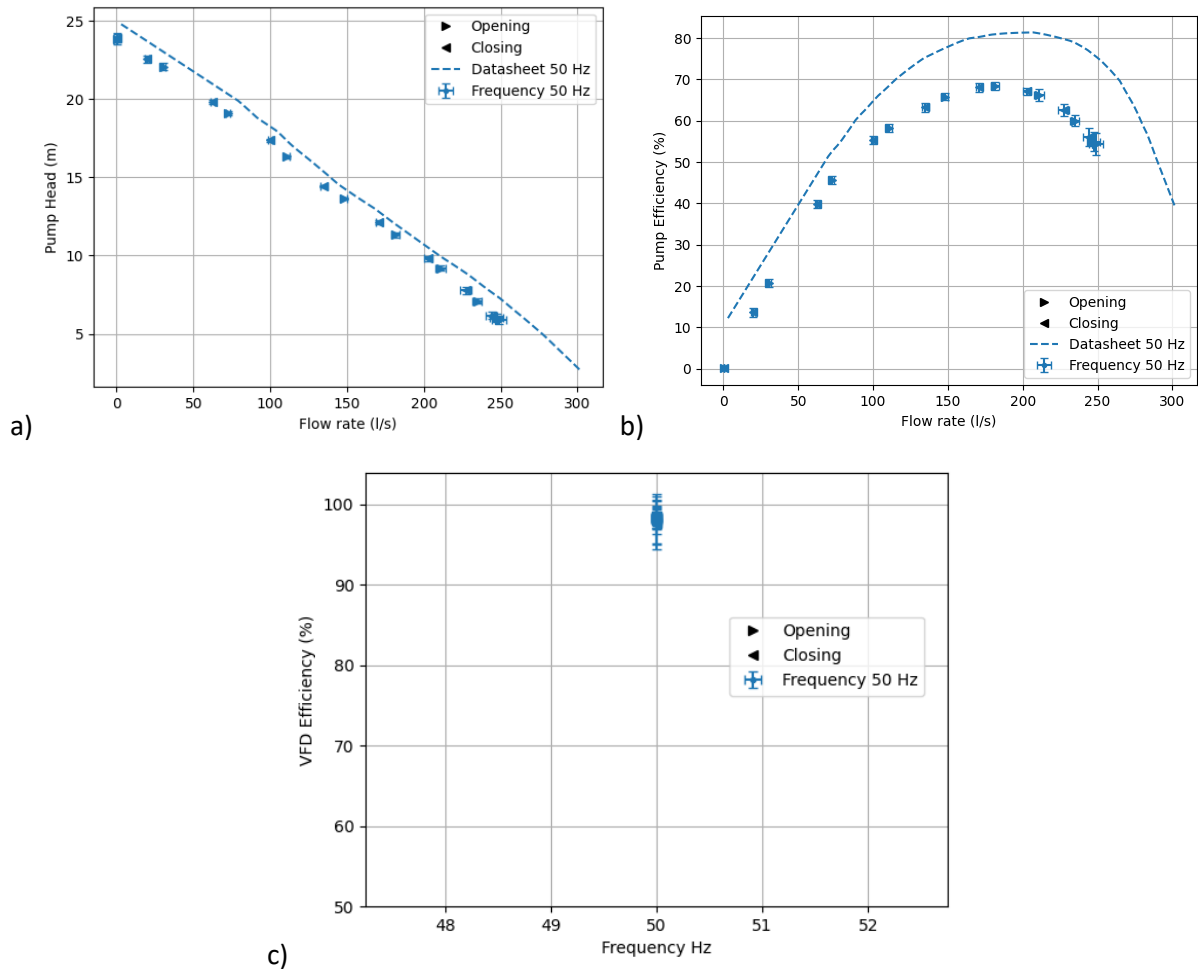


Figure 3.2: Experimental results of testing procedure n°3 compared to datasheet for the Hidrostral pump using a soft starter: (a) head-(flow rate) curve; (b) overall pump efficiency curve and (c) soft starter efficiency

4 Computational results

The computational results obtained based on a model calibration using Gekko solver (Calibration procedure n°2) are presented here, in combination with observations collected through Testing procedure n°3. The calibration procedure was applied on the bench results to provide parameters to the pump numerical model.

The obtained calibrated parameter values are given in Table 2. Running the developed model with these parameter values, leads to the results shown in Figure 4.1 for flow rate, head, overall pump efficiency and electric power. The outcomes of the computational model are found to agree very well with the experimental observations.

The maximum modelling absolute errors are of the order of 9 l/s, 1.4 kW and 8 pp for the flow rate, the electric power and the efficiency, respectively (Figure 4.2). The maximum errors on the flow rate and the electric power increase with the frequency (up to 9 l/s and 1.4 kW). In contrast, the maximum errors on the pump efficiency remain relatively constant (around 8 pp) when the frequency is varied.

In relative terms, the flow rate, the electrical power and the efficiency are reproduced by the computational model with a mean error of about 4%, 2.5 % and 2 pp, respectively (Figure 4.3). This highlights a particularly good model accuracy for predicting electric power and efficiency.

The computational model suits pretty well the Hidrostal pump. Explanation comes from the real operation of the Hidrostal pump that fit the modelled quadratic behaviour of the head and the torque with respect to the flow rate. The affinity law was forced during the calibration. Nevertheless, if the affinity exponents are considered as part of the parameters to be calibrated, the root mean square errors slightly decrease from those obtained when using the affinity law (Figure 4.3). The affinity exponents found by calibration are $\alpha = 0.9910$, $\beta = 2.0314$, $\gamma = 2.1316$.

An efficiency map of the Hidrostal pump is shown in Figure 4.4. The computed efficiency lumps the efficiencies of the motor and pump, while the effect of the losses in the VFD has been separated thanks to Testing procedure n°3.

a_{app}	b_{app}	c_{app}	d_{app}	e_{app}	f_{app}
-0.05672	-0.46863	1.16361	-0.01639	-0.07151	0.94495
R_s	R_r	L_{ss}	L_{sr}	L_{rr}	A_{fr}
0.01	0.01	3.87	3.80	3.86	0.08717
a	b	c	d	e	f
-0.03695	-0.45983	0.965985	-0.01559	-0.06880	0.66751

Table 2: Numerical model parameters identified in the calibration procedure with $c_Q = 0.5$

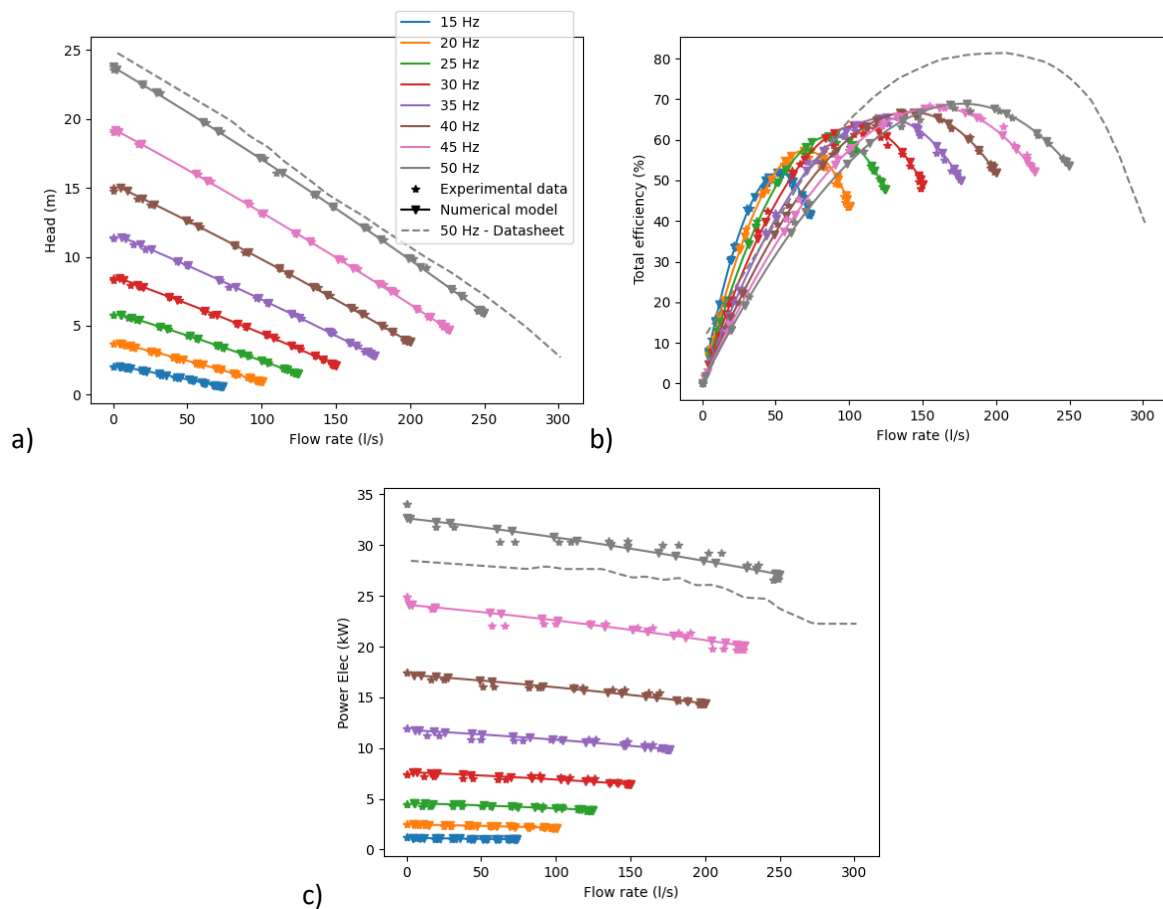


Figure 4.1: Comparison of the computational outcomes from calibration procedure n°2 with the experimental results of the testing procedure n°3 on the Hidrostal pump: (a) the head-(flow rate) curve; (b) the overall pump efficiency curve and (c) the electric power curve

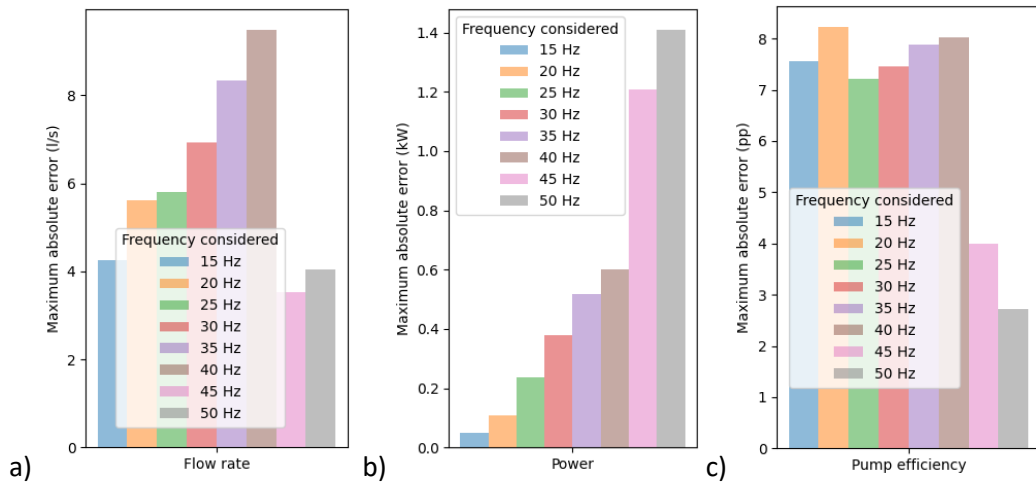


Figure 4.2: Maximum absolute errors of the computational outcomes ((a) the flow rate, (b) electric power and (c) pump efficiency) on Hidrostral pump from calibration procedure n°2 according to the frequency on experimental results obtained in testing procedure n°3

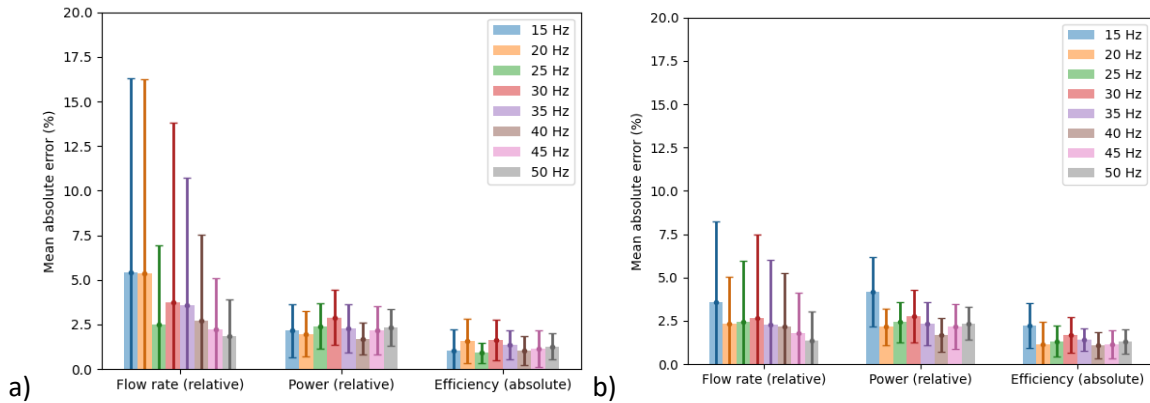


Figure 4.3: Distribution of the RMS error and standard deviation for flow rate, power consumption and total efficiency between numerical model and experimental results of the Hidrostral pump using calibration procedure n°2 on testing procedure n°3 (a) with affinity law or (b) without affinity law

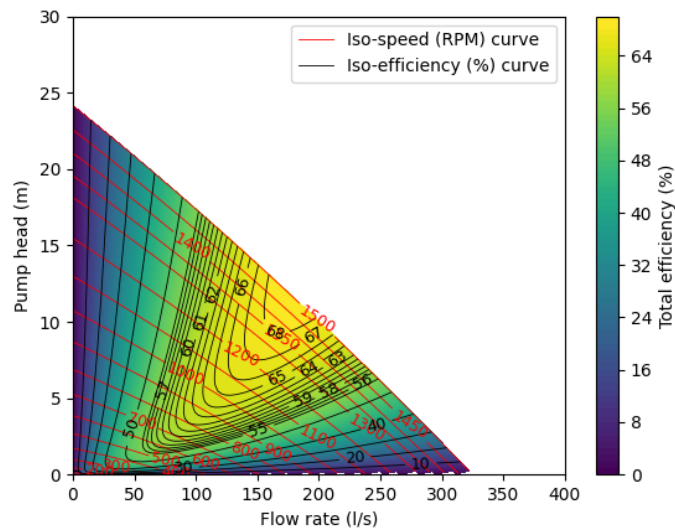


Figure 4.4: Efficiency map of the motor-pump assembly (Attention, it does not take into account the hydraulic efficiency of the suction/discharge system and the VFD efficiency) with BEP (11.5 m; 177 l/s) of the Hidrostral pump using calibration procedure n°3

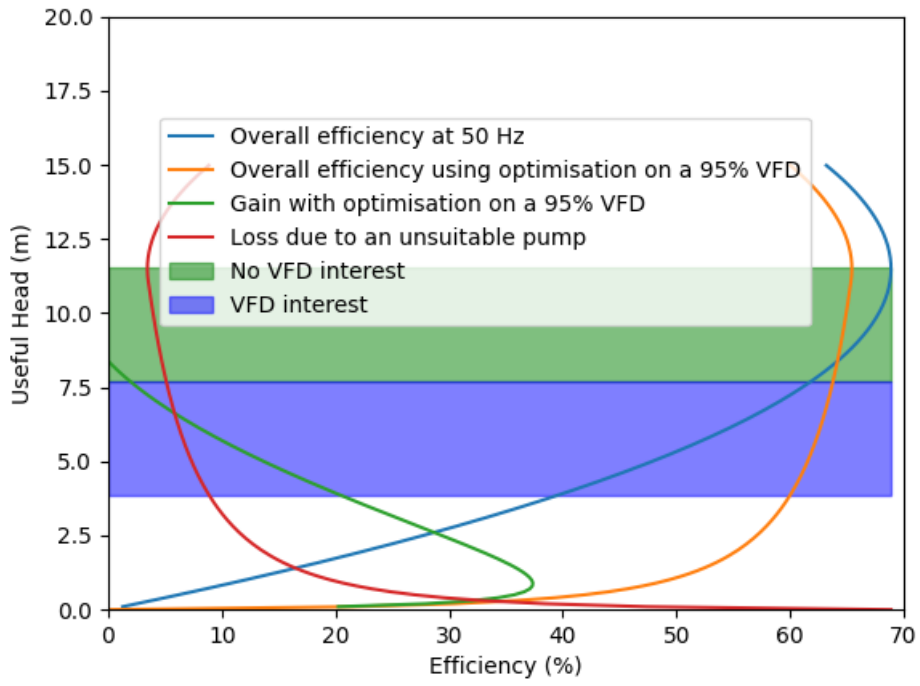


Figure 4.5: Comparison of efficiency using a full power pump or using a VFD with an optimised strategy for the Hidrostal pump

